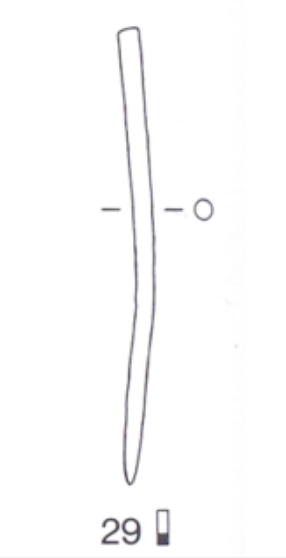
PIN WITHOUT HEAD HR-18152 - TIN BRONZE - LATE BRONZE AGE - SWITZERLAND

Artefact name Pin without head HR-18152

Authors Marianne. Senn (EMPA, Dübendorf, Zurich, Switzerland) & Christian. Degrigny (HE-Arc CR, Neuchâtel, Neuchâtel, Switzerland)

Url /artefacts/376/

The object



Credit HE-Arc CR.

Fig. 1: Tin bronze pin without head (after Rychner-Faraggi 1993, plate 74.29),

Description and visual observation

Description of the artefact Pin without head, light-brown patina typical of lake context (Fig. 1). Dimensions: L = 7,5cm; Ø = 3.3mm; WT = 4g.

Type of artefact Pin

Origin Hauterive - Champréveyres, Neuchâtel, Neuchâtel, Switzerland

Recovering date Excavation 1983-1985, object from layer 3 to 5

Chronology category Late Bronze Age

chronology tpq 1054 B.C.

chronology taq 1000 B.C.

Chronology comment Hallstatt B1 (1054/1037BC _ 1000BC)

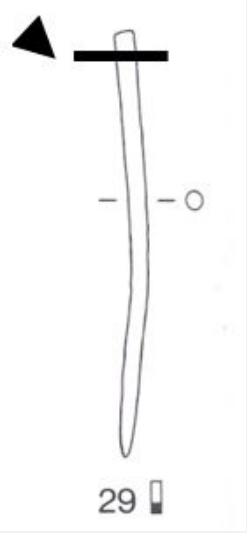
This work is licensed under CC BY-NC-ND 4.0

Burial conditions / environment	Lake
Artefact location	Laténium, Neuchâtel, Neuchâtel
Owner	Laténium, Neuchâtel, Neuchâtel
Inv. number	Hr 18152
Recorded conservation data	Not conserved

Complementary information

Nothing to report.

Study area(s)



Credit HE-Arc CR.

Fig. 2: Location of sampling area,

Binocular observation and representation of the corrosion structure

Stratigraphic representation: none.

MiCorr stratigraphy(ies) – Bi

Sample(s)

This work is licensed under CC BY-NC-ND 4.0

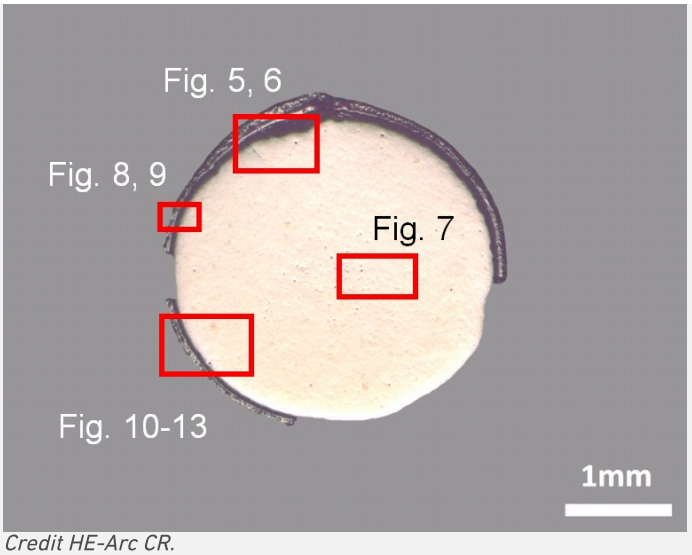


Fig. 3: Micrograph of the cross-section showing the location of Figs. 5 to 12,

Credit HE-Arc CR.

Description of sample	The cross-section is circular and is a complete section through the pin (Fig. 2). It is covered with a rather thin and regular (in thickness) corrosion crust. One third of the corrosion crust is missing (Fig. 3).
Alloy	Tin Bronze
Technology	Annealed after cold working
Lab number of sample	MAH 87-194
Sample location	Musées d'art et d'histoire, Genève, Geneva
Responsible institution	Musées d'art et d'histoire, Genève, Geneva
Date and aim of sampling	1987, metallography and corrosion characterisation

Complementary information

Nothing to report.

Analyses and results

Analyses performed:
Metallography (etched with ferric chloride reagent), Vickers hardness testing, XRF, ICP-OES, SEM/EDS, XRD, Raman spectroscopy.

Non invasive analysis

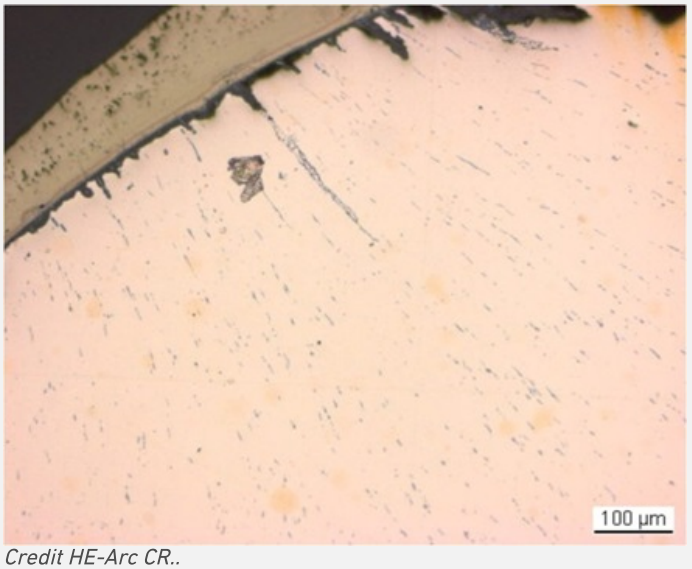
Metal

The remaining metal is a tin bronze and contains copper sulphide as well as heavy metal (Pb-rich) inclusions (Table 1, Figs. 5 and 6). Close to the surface of the remaining metal, copper sulphide inclusions are elongated and form rows (Fig. 5). The etched structure of the tin bronze shows polygonal grains; some of them are twinned (Fig. 7). In the centre of the sample and on the edges, the grains are smaller. The copper sulphide inclusions are located at the grain boundaries and in the grains. The average hardness of the metal is about HV1 110.

This work is licensed under CC BY-NC-ND 4.0

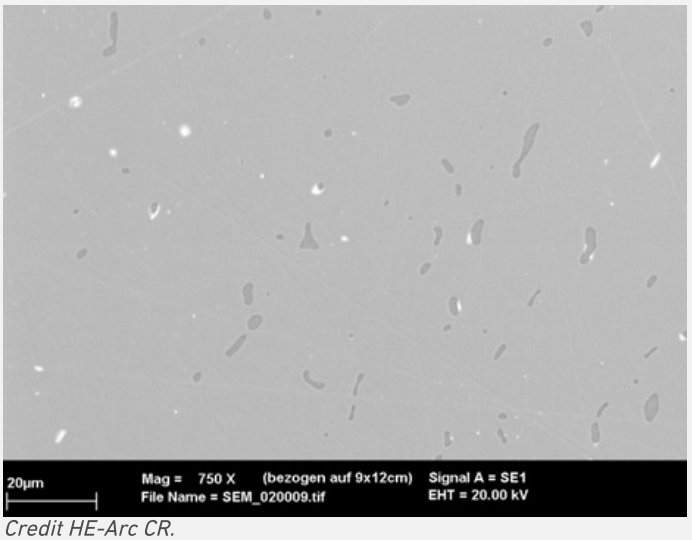
Elements	Cu	Sn	Pb	Sb	As	Ag	Fe	Ni	Co	Zn
mass%	89.22	9.57	0.34	0.26	0.19	0.15	0.09	0.05	0.06	0.05

Table 1: Chemical composition of the metal. Method of analysis: ICP-OES, Laboratory of Analytical Chemistry, Empa.



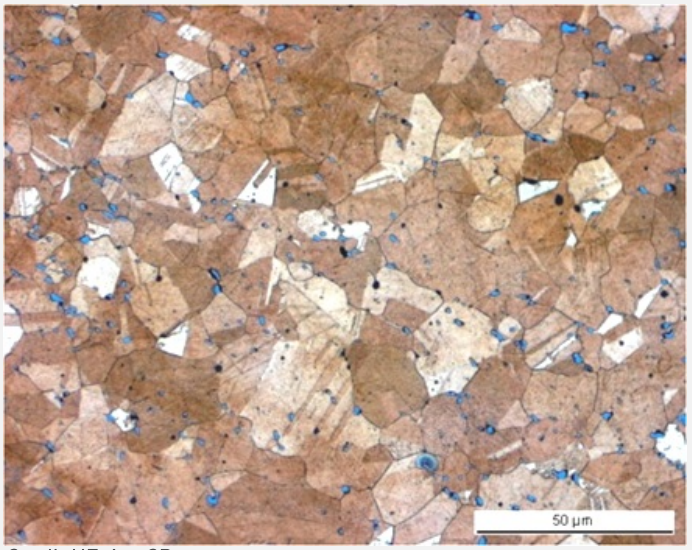
Credit HE-Arc CR..

Fig. 5: Micrograph of the metal sample from Fig. 3 (detail), unetched, bright field. Rows of elongated copper sulphide inclusions can be observed,



Credit HE-Arc CR.

Fig. 6: SEM image of the metal sample from Fig. 3 (detail), SE-mode. Elongated copper sulphide inclusions (dark-grey) are visible as well as heavy metal (Pb-rich) inclusions (white),



Credit HE-Arc CR.

Fig. 7: Micrograph of the metal sample from Fig. 3 (detail), etched, bright field. The metal shows a structure of polygonal and twinned grains. Copper sulphide inclusions are visible as blue spots,

This work is licensed under CC BY-NC-ND 4.0

Microstructure	Polygonal and twinned grains
First metal element	Cu
Other metal elements	Sn

Complementary information

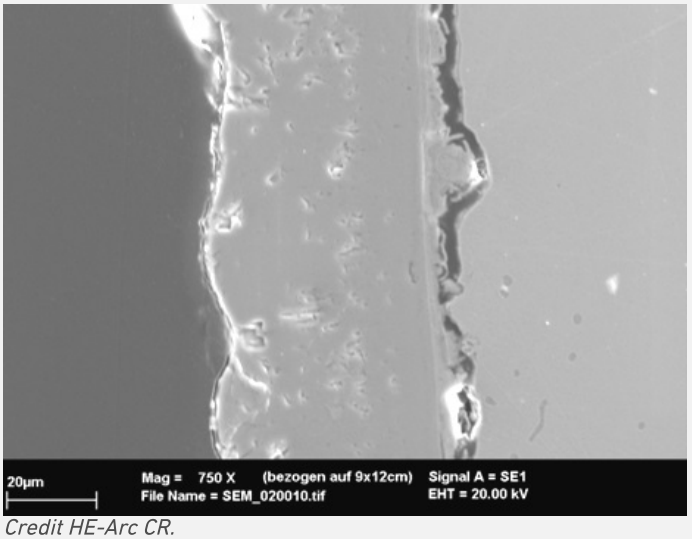
Nothing to report.

Corrosion layers

The corrosion crust is regular in thickness (100µm). One third is missing (Fig. 3). At the metal - corrosion crust interface, there is a crack showing that the latter has separated from the metal core along its whole length (Figs. 8 and 9). The corrosion crust can be divided into three distinct layers (CP1-3). Directly above the crack is a first dense but cracked and irregular inner layer (CP3, Figs. 8 and 9). In bright field it appears brown (Fig. 10), in polarised light dark brown (Fig. 11). It is separated from the adjacent layer by a clear line (Figs. 9 and 10). The second layer (CP2) is dense with little porosity (Figs. 8 and 9). In bright field it appears light brown (fig. 10), in polarised dark grey (Fig. 11). The third and outermost layer (CP1) appears light brown in bright field (Fig. 10), contains particles (Fig. 9) and is very porous (visible as golden reflections under polarized light, Fig. 11). The elemental chemical distribution of the SEM image selected reveals that the inner layer (CP3) is depleted in Cu, but rich in Sn,O and Si (Fig. 12 and Table 2) and its interface with the intermediate layer (CP2) could represent the limit of the original surface (Figs. 8 and 12). The second and third layer (CP2 and CP1) are Fe,Cu and S-rich (Fig. 12) and have a composition similar to chalcopyrite/$CuFeS_2$ (Table 2). This was confirmed by XRD. The particles (inclusions) have a composition similar to covelline or covellite/CuS (Table 2). Both chalcopyrite and covelline have been identified by Raman spectroscopy (Figs. 13 and 14).

Elements	S	Fe	Cu	O	Si	Sn	Total
CP1 and CP2	35	30	34	<	<	<	99
Particles in CP1	26	4.1	68	<	<	<	98
CP3	5.8	5.0	13	32	2	41	99

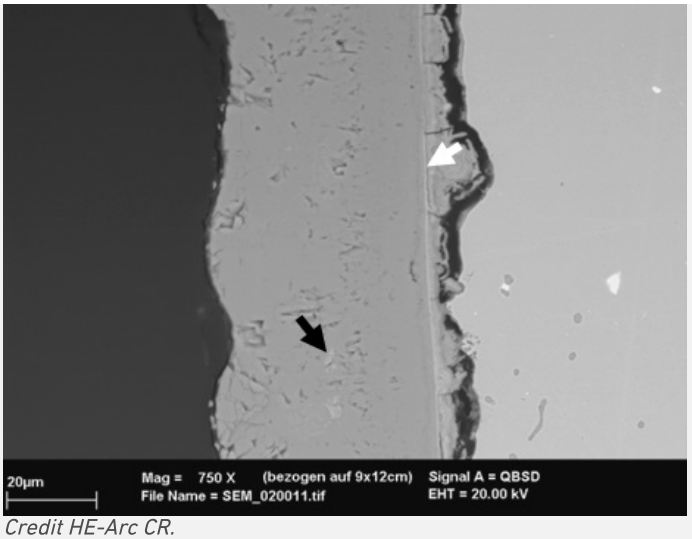
Table 2: Chemical composition (mass %) of the corrosion layer from Fig. 10. Method of analysis: SEM/EDS, Laboratory of Analytical Chemistry, Empa.



Credit HE-Arc CR.

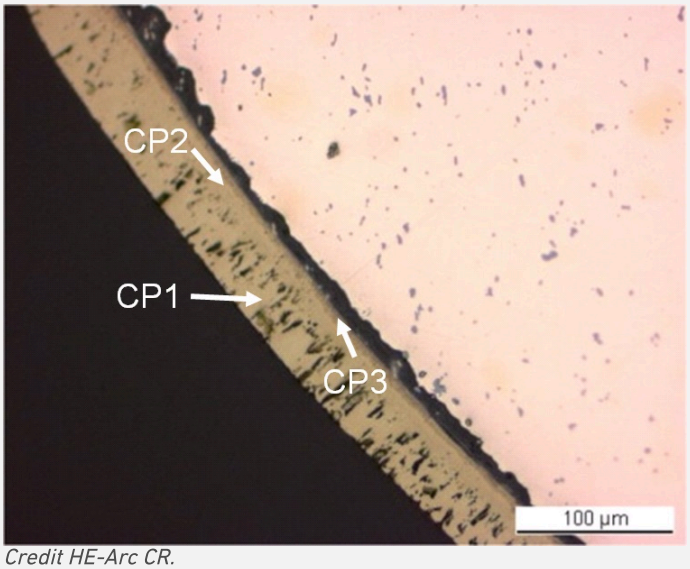
Fig. 8: SEM image of the metal sample from Fig. 3 (detail), SE -mode. The crack between the remaining metal and the corrosion layers is clearly visible,

This work is licensed under CC BY-NC-ND 4.0



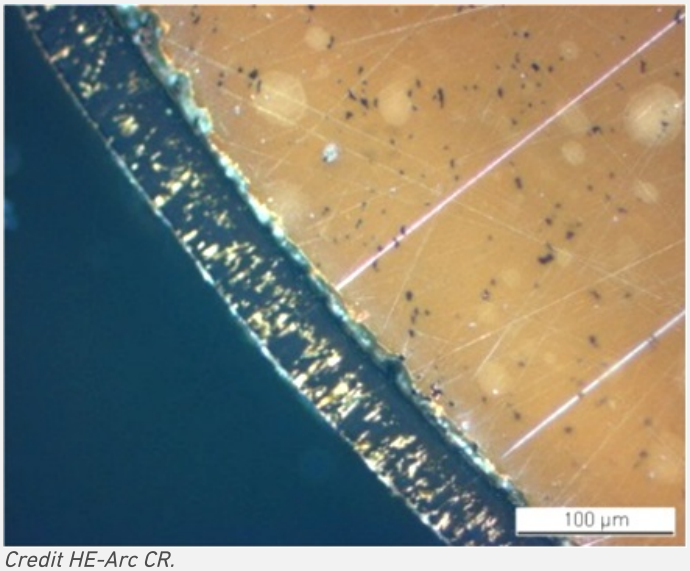
Credit HE-Arc CR.

Fig. 9: SEM image similar to Fig. 8, BSE-mode. A thin line is visible (white arrow) differentiating the inner Sn-rich layer from the intermediate and outer chalcopyrite layers. The latter contains bright covelline inclusions (black arrow) and pores,



Credit HE-Arc CR.

Fig. 10: Micrograph of the metal sample from Fig. 3 (detail) and corresponding to the stratigraphy of Fig. 4, unetched, bright field,



Credit HE-Arc CR.

Fig. 11: Micrograph similar to Fig. 10, polarised light,

This work is licensed under CC BY-NC-ND 4.0

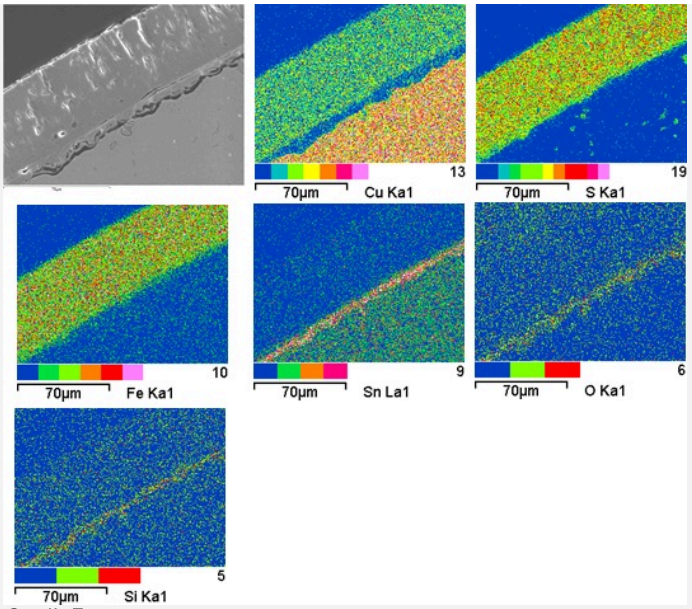


Fig. 12: SEM image and elemental chemical distribution of a selected area of Fig. 10 (rotated by 90°). Method of examination: SEM/EDS, Laboratory of Analytical Chemistry, Empa,

Credit Empa.

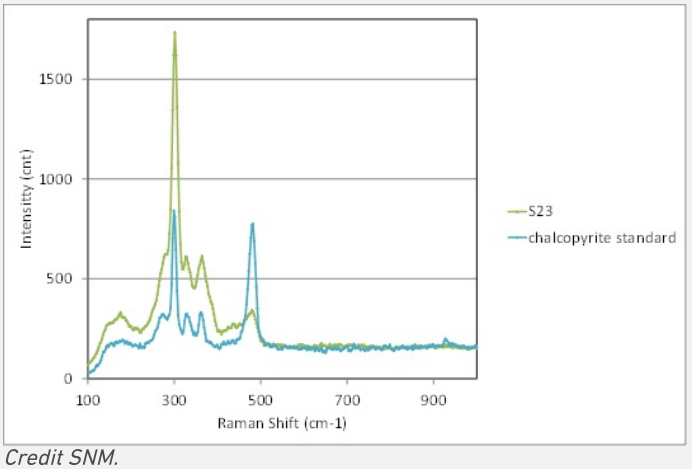


Fig. 13: Raman spectrum of the outermost layer (S23) of Fig. 9 compared to a chalcopyrite standard spectrum. Settings: laser wavelength 532nm, acquisition time 50s, 4 accumulations, filter D2 (0.75-0.8mW), hole 1000, slit 100, grating 600. Method of analysis: Raman spectroscopy, Lab of Swiss National Museum, Affoltern a. Albis ZH,

Credit SNM.

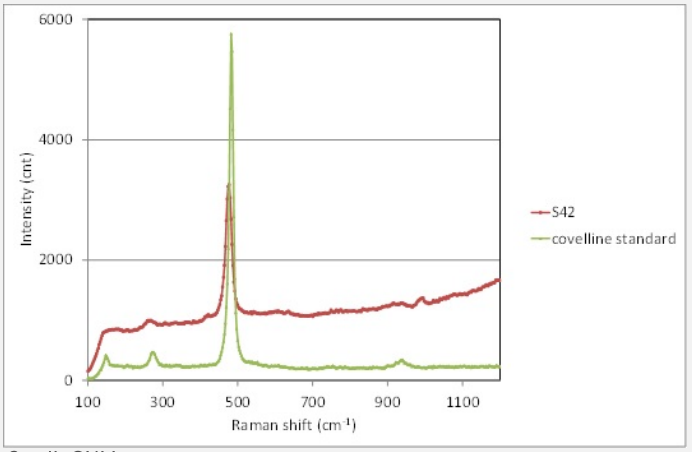


Fig. 14: Raman spectrum of the inclusions of the outermost layer (S42) of Fig. 9 compared to a covelline / covellite standard spectrum. Settings: laser wavelength 532nm, acquisition time 10s, 5 accumulations, D2 (0.75-0.8mW), hole 500, slit 80, grating 600. Method of analysis: Raman spectroscopy, Lab of Swiss National Museum, Affoltern a. Albis ZH,

Credit SNM.

Corrosion form	Uniform - pitting
Corrosion type	Type I (Robbiola)

Complementary information

Nothing to report.

This work is licensed under CC BY-NC-ND 4.0

MiCorr stratigraphy(ies) – CS

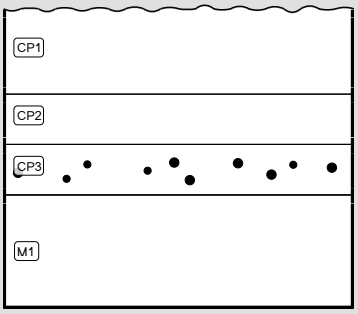


Fig. 4: Stratigraphic representation of the object in cross-section using the MiCorr application. This representation can be compared to Fig. 10, Credit HE-Arc CR.

Synthesis of the binocular / cross-section examination of the corrosion structure

Corrected stratigraphic representation: none.

Conclusion

The pin is made from tin bronze and has been annealed after cold working. It is covered with a regular, light-brown patina typical of lake context (Schweizer 1994). The inner, thin Sn-rich corrosion layer contains soil elements such as Si. The light-brown, thick intermediate and outer corrosion layers have the composition of chalcopyrite. This object was certainly abandoned rather quickly in an anaerobic, humid and S and Fe-rich environment, favouring the formation of the above mentioned compound. The limit of the original surface can be located between the chalcopyrite and the Cu depleted but Sn-rich inner corrosion layer. Thus, the corrosion is a type 1 according to Robbiola et al. 1998.

References

References on object and sample

References object

1. Rychner-Faraggi A-M. (1993) Hauterive – Champréveyres 9. Métal et parure au Bronze final. Archéologie neuchâteloise, 17 (Neuchâtel).
2. Hochuli, S. et al. (1988) SPM III Bronzezeit , Verlag Schweizerische Gesellschaft für Ur- und Frühgschichte Basel, 76-77, 379.

References sample

3. Empa Report 137 695/1991, P.O. Boll.
4. Rapport d'examen, Lab. Musées d'Art et d'Histoire, Geneva GE, 87-194 à 87-197.
5. Schweizer, F. (1994) Objets en bronze provenant de sites lacustre: de leur patine à leur biographie. In: L'œuvre d'art sous le regard des sciences (éd. Rinuy, A. and Schweizer, F.), 143-157.

References on analytic methods and interpretation

6. Robbiola, L., Blengino, J-M., Fiaud, C. (1998) Morphology and mechanisms of formation of natural patinas on archaeological Cu-Sn alloys, Corrosion Science, 40, 12, 2083-2111.

This work is licensed under CC BY-NC-ND 4.0

This work is licensed under CC BY-NC-ND 4.0